MAIAC Thermal Technique for Smoke Injection Height From MODIS

Alexei Lyapustin, Yujie Wang, Sergey Korkin, Ralph Kahn, and David Winker

***Abstract*— We present a new algorithm to derive smoke plume height (H^a) using the thermal contrast from the rising mixture of aerosol and emitted gases in the Moderate Resolution Imaging Spectroradiometer (MODIS) 11-μm channel. Validation shows good agreement with the wind-corrected Multi-angle Imaging SpectroRadiometer (MISR)-MISR Interactive Explorer (MINX) values, with about 60% of the MODIS Terra thermal retrievals within 500 m of MISR H^a and 450 m lower on average. The bias is expected because the thermal technique represents an effective rather than a top plume height from MISR MINX. The comparison of MODIS Aqua retrievals with Cloud-Aerosol LiDAR with Orthogonal Polarization (CALIOP) Cloud-Aerosol LiDAR and Infrared Pathfinder Satellite Observations (CALIPSO) shows similar statistics, with a standard deviation of 458 m for the mean plume height and 216 m lower on average. H^a is part of the Multi-Angle Implementation of Atmospheric Correction (MAIAC) MODIS Collection 6 suite of products (MCD19), accessible via the Land Product Distributed Active Archive Center (LP DAAC). Aerosol injection height is reported in the daily MAIAC atmospheric product MCD19A2 along with the cloud mask (CM), column water vapor, aerosol optical depth (AOD), AOD uncertainty, and aerosol type, at 1-km resolution on a global sinusoidal grid. Despite some limitations, the vastly increased coverage from MODIS observations makes it a valuable data set complementing the established MISR and CALIOP products.**

***Index Terms*— Atmosphere < methodologies and applications to, electromagnetics and remote sensing.**

I. Introduction

WILDFIRE smoke plume height (H^a) is an important parameter for constraining aerosol chemical transport models in GCMs. It determines whether emitted smoke is a localized phenomenon limited to the atmospheric boundary layer or is injected into a free troposphere and can travel long distances. Plume height information is required for modeling local and regional aerosol transport, air quality, and so on. Knowledge of the injection height is particularly important for modeling plume rise of energetic fires, which is associated with large uncertainties; model representations of small fires with low injection heights are much better constrained.

Plume height or "aerosol layer altitude," respectively, is currently available from two satellites: the Multi-angle Imaging SpectroRadiometer (MISR) aboard the NASA Terra satellite [1], [2] and the Cloud-Aerosol LiDAR with Orthogonal Polarization (CALIOP) aboard the Cloud-Aerosol LiDAR and Infrared Pathfinder Satellite Observations (CALIPSO) [3], [4]. Although these satellites provide planet-wide observations, they are limited in temporal frequency, with 16-day subspacecraft coverage for CALIOP and 9-day global coverage for MISR; as a result, many fires are missed. Although MISR plume heights are reported at 1.1-km horizontal resolution and CALIOP values are provided at up to 70 m, in a recent review of smoke injection height in large-scale atmospheric chemical transport models, Paugam *et al.* [5] state that "determination of the injection heights at spatiotemporal scales matching active fire observations" from the Moderate Resolution Imaging Spectroradiometer (MODIS) "is more likely to rely on injection height parameterizations" for many applications, due to the coverage limitations of MISR and CALIOP. Here, we present a new MODIS-based thermal technique for smoke injection height implemented in the Multi-Angle Implementation of Atmospheric Correction (MAIAC) algorithm [6]. The broad-swath MODIS instruments each cover the entire planet every 1–2 days. In this letter, we use the terms "injection height" and "plume height" interchangeably, though the latter is an approximation of the former near the source.

II. MAIAC Plume Height Algorithm

The recently described MAIAC algorithm [6] offers a unique infrastructure for smoke detection and characterization. It includes the following: 1) high-quality cloud and snow detection; the cloud mask (CM) algorithm includes detection of thermal hotspots based on modified [7]; 2) detection of absorbing smoke and dust aerosols. The smoke test is optimally integrated with cloud detection in a way that minimizes cloud leak and preserves most of the strong smoke plumes, which are usually filtered by CM [6], [8], [9]; and 3) aerosol optical depth (AOD) retrieval at high 1-km resolution.

Rising aerosol plumes from wildfires often display a "colder" brightness temperature (T_b), representing its effective height above ground, and creating T_b contrast with the

Manuscript received April 23, 2019; revised June 25, 2019; accepted August 16, 2019. Date of publication September 12, 2019; date of current version April 22, 2020. The work of A. Lyapustin was supported in part by the NASA Science of Terra, Aqua, SNPP under Grant 17-TASNPP17-0116; solicitation NNH17ZDA001N-TASNPP and in part by the NASAGeoCAPE Program. The works of Y. Wang and S. Korkin were supported by the NASA Science of Terra, Aqua, SNPP under Grant 17-TASNPP17-0116; solicitation NNH17ZDA001N-TASNPP. *(Corresponding author: Alexei Lyapustin.)*

A. Lyapustin and R. Kahn are with the Laboratory for Atmospheres, NASA Goddard Space Flight Center, Greenbelt, MD 20771 USA (e-mail: alexei.i.lyapustin@nasa.gov).

Y. Wang is with JCET, University of Maryland Baltimore County, Baltimore, MD 21201 USA.

S. Korkin is with GESTAR Universities Space Research Association, Columbia, MD 21046 USA.

D. Winker is with the NASA Langley Research Center, Hampton, VA 23666 USA.

Color versions of one or more of the figures in this letter are available online at http://ieeexplore.ieee.org.

Digital Object Identifier 10.1109/LGRS.2019.2936332

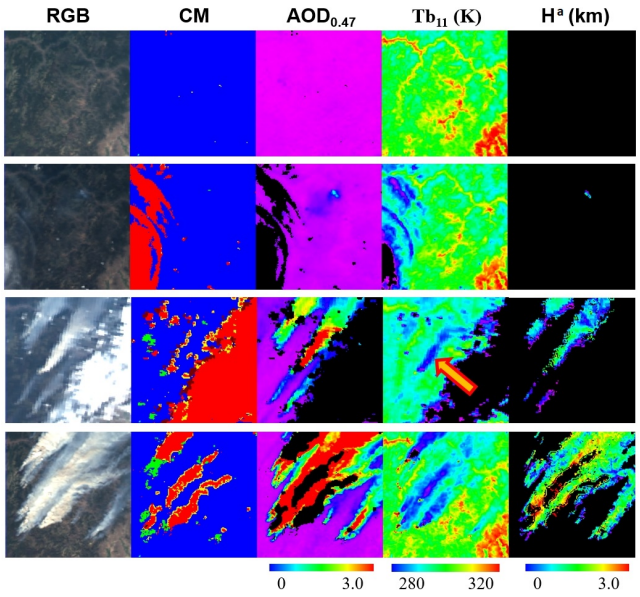

Fig. 1. Illustration of smoke plume height retrieval from MODIS for the Rocky Mountains wildfires of summer 2008. The columns show the MODIS TOA RGB image, MAIAC CM, AOD, 11-μm brightness temperature (T_b), and plume height above ground. The CM legend is as follows: Clear, Cloud, Shadow, and Detected fire. Each row corresponds to a different day of 2008, specifically 190, 191, 202, and 224. An arrow identifies the thermal contrast created by the rising smoke plume on day 202.

neighbor smoke-free ground pixels (ΔT_b). The MAIAC smoke detection allows us to implement a simple aerosol plume height algorithm for pixels with detected smoke based on ΔT_b, under an assumed atmospheric temperature profile or an average lapse rate. Fig. 1 shows an illustration for the Rocky Mountain wildfires during summer 2008. The columns show the MODIS top-of-atmosphere (TOA) RGB image, MAIAC CM, AOD at 470 nm (AOD0.47), 11-μm brightness temperature (T_b), and the derived plume height for an assumed lapse rate of 6.5° km^{-1}. The green color in the CM panel shows detected fire hotspots. Each row corresponds to a different day of 2008, specifically 190, 191, 202, and 224. An arrow identifies the thermal contrast in the MODIS 11-μm channel (band 31) created by the rising smoke plume on day 202. Several strong plumes are easily visible on day 224 in TOA RGB, AOD, and T_b images.

The fine-mode aerosol particles generated by fires are not visible in the 11-μm channel. The thermal contrast is created by several other physical mechanisms: the main one is the absorption by gases entrained in the rising smoke plume and the re-emission from the effective plume altitude. Although 11 μm is considered an atmospheric window channel, there is absorption by carbon dioxide (CO_2), nitrous oxide (NO_2), ammonia (NH_3), methane (CH_4), water vapor, and other gases released during combustion. Normally, absorption by these gases under background conditions is ~7%–10%. Within wildfire plumes, the concentrations of these gases can be much higher than in the background atmospheric column, creating a significant absorption. Next, wildfires often release a considerable amount of water vapor that can condense into 5- to 10-μm liquid droplets at the top of the aerosol plume. The resulting pyrocumulus clouds provide another source of the thermal contrast. Other mechanisms that do not affect the current results include surface irradiance reduction by the smoke and cooling of the surface below compared with the smoke-free areas [10].

MAIAC smoke detection [8], [11] is the key feature of the algorithm that allows MAIAC to bypass cloud detection, retain most of the strongest plumes, and provide AOD at 1-km resolution. The smoke height is evaluated for a pixel (i, j) with detected smoke if 1) the AOD at 0.47 μm is sufficiently high ($\geq$0.8); 2) an estimate of the ground brightness temperature T_{bG} for the smoke-free land surface is available; and 3) $\Delta T_b = T_{bG} - T_{b,ij} > 0$. When all three conditions are met, MAIAC computes the plume height assuming a fixed lapse rate of 6.5° km^{-1}, $H^a = \Delta T_b/6.5$ (km).

The ground brightness temperature in the MAIAC algorithm is computed as an average value for each 25 × 25 km^2 block using cloud- and smoke-free pixels. If T_{bG} for the block containing pixel (i, j) is not available, we compute T_{bG} as a weighted average from a larger mesoscale (150 km) area, where the weights are defined as an inverse squared distance. To account for the surface height variation in nonflat terrain, we compute T_{bG} for five surface-height bins, in increments of 0.5 km: 0–0.5 km, ... 2–2.5 km, and use the appropriate T_{bG} bin corresponding to the pixel (i, j) surface height.

The described thermal technique has several limitations. First, the emitted gas concentrations decrease over time, and with distance from the source of burning, due to dilution and chemical reactions in the gas phase, including oxidation, the formation of secondary organic aerosol, heterogeneous reactions, and coatings created on the primary organic, black- and brown carbon aerosol particles. The decrease in the absorbing gas concentration leads to an increased "warmer" surface contribution to the TOA 11-μm radiance signal, effectively pushing the "weighting function" toward the surface. The resulting reduction in thermal contrast could be interpreted incorrectly by this technique as a decrease in the plume height. This phenomenon limits the application of the thermal technique to a certain "dissipation" distance from the source. Second, our approach does not work when the smoke area is very large and T_{bG} cannot be estimated reliably. Finally, the thermal technique is not designed for small fires, having low emission of absorbing gases and lack of thermal contrast. The empirical threshold AOD >0.8 helps filter these cases.

The algorithm presented also uses two main simplifications. The first is the use of the average lapse rate of 6.5° km^{-1} instead of an atmospheric temperature profile from climate or weather forecast models. This simplification was adopted initially because 1) in the absence of a dense radiosonde network, the profiles from different models may not agree, indicating general uncertainty and 2) the MODIS operational processing uses forecast, whereas reanalysis available several hours later would provide more accurate atmospheric profiles. Thus, our approach allows an experienced user to rescale the H^a value back to the ΔT_b contrast and derive a more accurate aerosol height estimate with a user-selected profile. If used as is, MAIAC H^a accuracy is somewhat reduced and can contain regional and seasonal biases. The second simplification is the use of the brightness temperature for

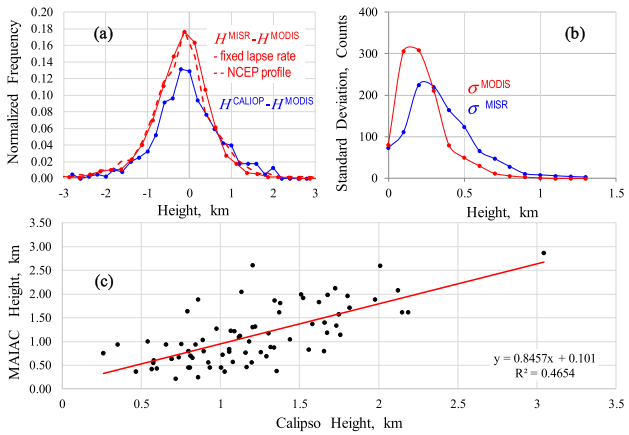

Fig. 2. (a) Histograms of MODIS Terra-MISR and MODIS Aqua—CALIOP—5-km plume height differences. (b) Standard deviations of the retrieved plume heights for MODIS Terra and MISR. (c) Scatterplot of MODIS Aqua—CALIOP plume heights averaged over transects of individual fires.

the background characterization, which assumes the surface emissivity ($\varepsilon = 1$). The emissivity in MODIS band 31 (11 μm) ranges from 0.92 to 1 [12] and is rather stable over vegetated surfaces ($\varepsilon \sim$ 0.97–0.98) where fires occur. Lower values are found over deserts and semiarid/arid areas. At a surface temperature $T = 300$ K with $\varepsilon \sim 0.975$, the assumption $\varepsilon = 1$ will bias T_{bG} by approximately 1.7 K and reduce the retrieved height by about 260 m. Finally, the absorption of the water vapor emitted by fire can add to uncertainty in our approach.

III. Comparison With MISR and CALIOP Data

A specialized MISR Interactive Explorer (MINX) program uses optical parallax along with the operator input of source location, wind direction, and plume area to derive H^a, e.g. [2]. Wind-corrected plume heights from MISR MINX have an accuracy of 250–500 m. We compared MAIAC H^a from MODIS Terra with the coincident MISR-MINX values for 1089 plumes over North America from 2000 to 2008 [13] (https://misr.jpl.nasa.gov/getData/accessData/MisrMinxPlumes2/). Statistical analysis of these cases is shown in Fig. 2 in histograms of (a) the H^{MISR}-H^{MODIS} height difference distribution ("fixed lapse rate" shown by the red solid line) and (b) the standard deviations of retrieved heights for each algorithm. The MAIAC values are lower by about 200 m at the peak of the histogram and by 448 m on average. In addition to MAIAC's systematic bias from the neglect of surface emissivity, the effective plume heights from MAIAC are expected to be lower than the MISR values, which generally relate to plume-top (though distribution of heights giving some indication of plume vertical extent is usually obtained [1]). About 59.3% of the MAIAC plume heights are found within ±500 m of the MISR-MINX values. The MAIAC-retrieved plume heights show smaller standard deviation, $\sigma_H = 179$ m, versus 300 m for MISR. This comparison indicates good agreement, given the uncertainties of both data sets, including a singularity in the MISR approach when the plume and satellite orbit directions closely align [2], simplifications in the MAIAC technique, and differences in the vertical sampling of these methods. It is also worth mentioning that generating the MISR MINX data set for 1089 fires required operator fire detection and other input, whereas the MAIAC retrievals were available automatically with the exception of small fires.

In addition, MAIAC H^a values from MODIS Aqua were compared with the data from CALIOP on the CALIPSO satellite that orbit together in the A-train constellation. We used the version 4.10 "lidar level 2 cloud and aerosol layer products" reported at 5-km resolution. Similar to [14], we find that the MAIAC heights are significantly lower than the CALIOP layer top altitude, even when a single layer was reported. Due to CALIOP sensitivity to high-altitude aerosol layers, extinction-weighted values, as in [14], did not yield good comparisons either. Better agreement is obtained when the CALIOP "height" is derived as the average between the reported layer top and the base altitudes, corrected for the surface elevation. For multi-layer cases, the average height of the optically thickest layer with the highest "Feature_Optical_Depth_532" is used. The CALIOP data were excluded when the feature optical depth was a factor of ≥3 larger or smaller than the corresponding MAIAC AOD value. For each 5-km CALIOP box, the MAIAC H^a value is represented by the maximal retrieved height within the nested 1-km MAIAC grid. The colocation error due to the 1–2 min overpass time difference between MODIS Aqua and CALIPSO amounts to ±5 km. To mitigate uncertainties from colocation and other sources, we also compare the values averaged over the transect length of individual plumes. To mitigate the MAIAC uncertainties from ground brightness temperature characterization, this analysis was limited to well-defined smoke plumes close to the emission source. These were identified based on the detected thermal hotspots and a sharp boundary in the MAIAC AOD, dropping to the background level within a ±75-km region. This automated analysis over North America from 2006 to 2017 identified 404 5-km boxes and 76 individual plumes with matched MODIS Aqua—CALIOP retrievals.

The results from this comparison are shown in Fig. 2(a) and (c). As with the MISR MINX results, MAIAC thermal H^a agrees with the CALIPSO values to within measurement uncertainties, on average 216 m lower, with a standard deviation of 458 m for the plume-averaged transects. When considering the larger statistics for 5-km boxes, the standard deviation is higher (851 m). Previous studies found the CALIPSO plume-top heights to be generally higher than MISR, due primarily to differences in instrument sensitivities to very thin aerosol [15], [16]. The current analysis applies a definition of the CALIPSO plume height that averages the layer top and bottom heights. This significantly lowers the effective CALIPSO values and accounts for MAIAC H^a appearing on average 458 m below MISR, but only 216 m below CALIPSO.

To evaluate the effect of the fixed lapse rate assumption, we recalculated MAIAC H^a using the National Center for Environmental Predictions (NCEP) temperature profiles [17] available as part of the MODIS ancillary data set. The result of the comparison with the MISR MINX values is presented in Fig. 2(a) by the dashed line. It shows that indeed, the use

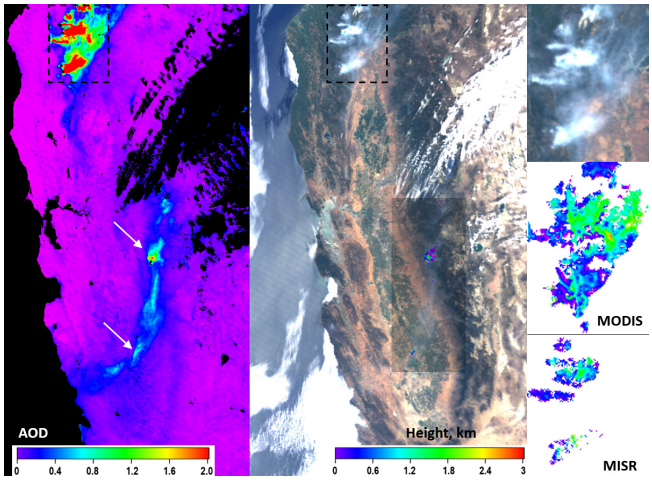

Fig. 3. Illustration of retrievals for California fires on July 29, 2008. (Left to right) MAIAC AOD, MODIS Terra RGB image, and MODIS Terra and MISR MINX injection height retrievals for Northern California. Arrows in the AOD image indicate the locations of additional MAIAC height retrievals for the California Central Valley that appear as darker overlays in the MODIS RGB image but were not digitized for the MISR MINX database.

of the realistic temperature profiles narrows the histogram of the MODIS–MISR height difference by about 10% in approximately half of all cases, thus improving the agreement. On the other hand, we did not observe an improved agreement with CALIPSO, which may be explained by several factors, including our definition of CALIPSO height, a rather coarse $1^\circ \times 1^\circ$ resolution of the NCEP profiles, which creates uncertainty over nonflat terrains, and the fundamental differences in the sensitivities of the two instruments.

IV. Spatial Coverage

To evaluate retrieval coverage, we compared the plume height retrieval statistics from MODIS Terra and MISR over North America for 2018. When considering the area covered by valid MISR MINX retrievals, the statistics are nearly identical: 25087 versus 25002 pixels with valid plume heights from MISR and MODIS Terra, respectively. MAIAC does not provide retrievals for some small fires captured by MISR, but as MAIAC reports the large fires over a greater area, the total MAIAC retrieval count is comparable to that of MISR. An example of such retrievals for Northern California on July 29, 2008 is shown in Fig. 3.

For the area covered by the MISR field of view (380-km swath width), MAIAC reports about a factor of 20 more plume height retrievals than MISR. The difference mostly represents the transported smoke far from the emission sources that the MISR-MINX operator most likely did not choose to digitize, but were nevertheless captured by the automatic MODIS algorithm. A separate validation of these retrievals with CALIOP data shows a lack of correlation in general, although about 20% of the data are in a good agreement. Because at present we cannot identify which MAIAC retrievals have a good quality in places where neither MISR nor CALIOP validation data are available, the use of this height product for the transported smoke is not recommended. It should be mentioned that the MISR MINX technique can be applied to the transported smoke, in addition to the current focus on the rising plumes from active fires. This analysis, therefore, shows that the current coverage of well-understood thermal MODIS Terra retrievals and MISR for the active fire plumes is very similar per unit area.

For the full MODIS swath (2330 km), the coverage difference with MISR grows in proportion to the area observed. It is interesting to note that the Aqua record features about 60% more detected hotspots by MAIAC and 14% more smoke height retrievals than Terra. This is consistent with the expected increase in fire energy from late morning to early afternoon. In summary, with the exception of small fires, the MAIAC MODIS provides reliable retrievals with similar coverage per unit area to that of MISR. However, it offers more retrievals due to the larger MODIS swath width, and the coverage is increased further as there are two MODIS sensors on orbit.

V. Conclusion

We present a new algorithm to derive smoke plume height using the thermal contrast created by the rising mixture of aerosol and emitted gases in the MODIS 11-μm channel. The thermal technique is simple and robust once clouds and smoke aerosol are reliably detected by the MAIAC MODIS processing. Validation shows a good agreement with the wind-corrected MISR-MINX values, with about 60% of the MAIAC retrievals within 500 m of MISR H^a, and skewed 450 m lower on average. The bias is expected in part because the thermal technique represents effective rather than peak-weighted plume height, and in part because MAIAC currently neglects nonunit surface emissivity. CALIOP validation of the MODIS Aqua retrievals shows similar statistics, namely, underestimation on average by 216 m with the standard deviation of 458 m for plume-averaged transects. The validation also shows that the retrievals are of comparable quality to MISR MINX for rising plumes in the proximity of active fires, but they are not as reliable for transported smoke.

The MAIAC MODIS Collection 6 processing has been completed and its product suite (MCD19) is accessible via the Land Product Distributed Active Archive Center (LP DAAC). The aerosol injection height is reported in the daily MAIAC atmospheric product MCD19A2 along with the CM, column water vapor, AOD, AOD uncertainty, and aerosol type, at 1-km resolution on a global sinusoidal grid. The reported H^a can either be used directly or recomputed using user-specified temperature profiles, for example, from the MERRA2 reanalysis (https://gmao.gsfc.nasa.gov/reanalysis/MERRA-2/). The MERRA-2 profiles and MODIS land surface emissivity, which recently became available from the MODIS Aqua MYD21 product [12] at 1-km resolution, will be implemented in the next version of the MAIAC algorithm. To exclude the transported smoke and ensure good quality of retrievals, we currently recommend to use H^a within ~75–150 km from the detected thermal hotspots as reported in the MAIAC quality assurance (QA) flag in the MCD19A2 product.

Although there are certain limitations to the technique presented, as discussed in Section II, the vastly increased coverage proportional to the observation coverage and at least partial representation of the diurnal cycle from the

∼10:30 A.M. (Terra) and ∼1:30 P.M. (Aqua) MODIS observations makes it a valuable data set complementing the established MISR and CALIOP products. The technique is generic and will be extended to the Suomi-NPP and J1 VIIRS measurements. A prototype algorithm has also been developed for the geostationary AHI-8 HIMAWARI data.

ACKNOWLEDGMENT

The following data sets were used in this letter.

1) "MAIAC MODIS atmospheric products (MCD19A2)," doi:10.5067/MODIS/MCD19A2.006.
2) "MISR MINX Plume Height," https://misr.jpl.nasa.gov/getData/accessData/MisrMinxPlumes2/.
3) "CALIOP v4.10 "Lidar Level 2 Cloud and Aerosol Layer Products," doi:10.5067/CALIOP/CALIPSO/LID_L2_05kmALay-Standard-V4-20.

REFERENCES

[1] R. A. Kahn, W.-H. Li, C. Moroney, D. J. Diner, J. V. Martonchik, and E. Fishbein, "Aerosol source plume physical characteristics from space-based multiangle imaging," *J. Geophys. Res.*, vol. 112, Jun. 2007, Art. no. D11205. doi: 10.1029/2006JD007647.

[2] D. L. Nelson, M. J. Garay, R. A. Kahn, and B. A. Dunst, "Stereoscopic height and wind retrievals for aerosol plumes with the MISR interactive explorer (MINX)," *Remote Sens.*, vol. 5, pp. 4593–4628, Sep. 2013. doi: 10.3390/rs5094593.

[3] D. M. Winker, M. A. Vaughan, A. Omar, Y. Hu, and K. A. Powell, "Overview of the CALIPSO mission and CALIOP data processing algorithms," *J. Atmos. Ocean. Technol.*, vol. 26, no. 11, pp. 2310–2323, Nov. 2009. doi: 10.1175/2009JTECHA1281.1.

[4] M. Labonne, F.-M. Breon, and F. Chevallier, "Injection height of biomass burning aerosols as seen from a spaceborne LiDAR," *Geophys. Res. Lett.*, vol. 34, no. 11, Jun. 2007, Art. no. L11806. doi: 10.1029/2007GL029311.

[5] R. Paugam, M. Wooster, S. Freitas, and M. Val Martin, "A review of approaches to estimate wildfire plume injection height within large-scale atmospheric chemical transport models," *Atmos. Chem. Phys.*, vol. 16, pp. 907–925, Jan. 2016. doi: 10.5194/acp-16-907-2016.

[6] A. Lyapustin, Y. Wang, S. Korkin, and D. Huang, "MODIS collection 6 MAIAC algorithm," *Atmos. Meas. Techn.*, vol. 11, no. 10, pp. 5741–5765, 2018.

[7] L. Giglio, W. Schroeder, and C. O. Justice, "The collection 6 MODIS active fire detection algorithm and fire products," *Remote Sens. Environ.*, vol. 178, pp. 31–41, Jun. 2016. doi: 10.1016/j.rse.2016.02.054.

[8] A. Lyapustin, S. Korkin, Y. Wang, B. Quayle, and I. Laszlo, "Discrimination of biomass burning smoke and clouds in MAIAC algorithm," *Atmos. Chem. Phys.*, vol. 12, pp. 9679–9686, Oct. 2012. doi: 10.5194/acp-12-9679-2012.

[9] I. Veselovskii *et al.*, "Characterization of forest fire smoke event near Washington, DC in summer 2013 with multi-wavelength lidar," *Atmos. Chem. Phys.*, vol. 15, pp. 1647–1660, Feb. 2015. doi: 10.5194/acp-15-1647-2015.

[10] J. Zhang, J. S. Reid, M. Christensen, and A. Benedetti, "An evaluation of the impact of aerosol particles on weather forecasts from a biomass burning aerosol event over the Midwestern United States: Observational-based analysis of surface temperature," *Atmos. Chem. Phys.*, vol. 16, pp. 6475–6494, May 2016. doi: 10.5194/acp-16-6475-2016.

[11] A. Lyapustin *et al.*, "Multiangle implementation of atmospheric correction (MAIAC): 2. Aerosol algorithm," *J. Geophys. Res.*, vol. 116, Feb. 2011, Art. no. D03211. doi: 10.1029/2010JD014986.

[12] G. C. Hulley and S. J. Hook, "Generating consistent land surface temperature and emissivity products between ASTER and MODIS data for Earth science research," *IEEE Trans. Geosci. Remote Sens.*, vol. 49, no. 4, pp. 1304–1315, Apr. 2011. doi: 10.1109/TGRS.2010.2063034.

[13] M. Val Martin, J. A. Logan, R. A. Kahn, F. Y. Leung, D. L. Nelson, and D. J. Diner, "Smoke injection heights from fires in North America: Analysis of 5 years of satellite observations," *Atmos. Chem. Phys.*, vol. 10, pp. 1491–1510, Feb. 2010. doi: 10.5194/ACP-10-1491-2010.

[14] M. G. Tosca, J. T. Randerson, C. S. Zender, D. L. Nelson, D. J. Diner, and J. A. Logan, "Dynamics of fire plumes and smoke clouds associated with peat and deforestation fires in Indonesia," *J. Geophys. Res.*, vol. 116, Apr. 2011, Art. no. D08207. doi: 10.1029/2010JD015148.

[15] R. A. Kahn *et al.*, "Wildfire smoke injection heights: Two perspectives from space," *Geophys. Res. Lett.*, vol. 35, Feb. 2008, Art. no. L04809. doi: 10.1029/2007GL032165.

[16] V. J. B. Flower and R. A. Kahn, "Assessing the altitude and dispersion of volcanic plumes using MISR multi-angle imaging from space: Sixteen years of volcanic activity in the Kamchatka Peninsula, Russia," *J. Volcanology Geothermal Res.*, vol. 337, pp. 1–15, May 2017. doi: 10.1016/j.jvolgeores.2017.03.010.

[17] E. Kalnay, M. Kanamitsu, and W. E. Baker, "Global numerical weather prediction at the national meteorological center," *Bull. Amer. Meteorolog. Soc.*, vol. 71, pp. 1410–1428, Oct. 1990.